Clim. Past Discuss., 6, 369–384, 2010
www.clim-past-discuss.net/6/369/2010/

Climate of the Past Discussions

This discussion paper is/has been under review for the journal Climate of the Past (CP).
Please refer to the corresponding final paper in CP if available.

Solar-forced shifts of the Southern Hemisphere Westerlies during the late Holocene

V. Varma[1], M. Prange[1,2], F. Lamy[2,3], U. Merkel[2], and M. Schulz[1,2]

[1]Dept. of Geosciences, Univ. of Bremen, Klagenfurter Strasse, 28334 Bremen, Germany
[2]MARUM – Center for Marine Environmental Sciences, Univ. of Bremen, Leobener Strasse, 28359 Bremen, Germany
[3]Alfred Wegener Institute for Polar and Marine Research, 27568 Bremerhaven, Germany

Received: 18 March 2010 – Accepted: 23 March 2010 – Published: 31 March 2010

Correspondence to: V. Varma (vvarma@marum.de)

Published by Copernicus Publications on behalf of the European Geosciences Union.

Abstract

The Southern Hemisphere Westerly Winds (SWW) constitute an important zonal circulation that influences large-scale precipitation patterns and ocean circulation. Variations in their intensity and latitudinal position have been suggested to exert a strong influence on the CO_2 budget in the Southern Ocean, thus making them a potential factor affecting the global climate. In the present study, the possible influence of solar forcing on SWW variability during the late Holocene is addressed. It is shown that a high-resolution iron record from the Chilean continental slope (41° S), which basically reflects changes in the position of the SWW, is significantly correlated with reconstructed solar activity. In addition, solar sensitivity experiments with a comprehensive global climate model (CCSM3) are carried out to study the response of SWW to solar variability. Taken together, the proxy and model results strongly suggest that centennial-scale periods of lower (higher) solar activity caused equatorward (southward) shifts of the SWW during the past 3000 years.

1 Introduction

The Southern Hemisphere Westerly Winds (SWW) constitute an important zonal circulation system that dominates the dynamics of Southern Hemisphere mid-latitude climate (e.g. Thresher, 2002; Shulmeister et al., 2004). Furthermore, they influence the global ocean circulation through wind-driven upwelling of deep water in the Southern Ocean (Toggweiler and Samuels, 1995; Kuhlbrodt et al., 2007; Sijp and England, 2009) and through the impact on the Indian-Atlantic Ocean water exchange by Agulhas leakage (Sijp and England, 2009; Biastoch et al., 2009). Moreover, the SWW may play a significant role in the global climate system through the control of the CO_2 budget in the Southern Ocean (Toggweiler et al., 2006; Anderson et al., 2009). Therefore, understanding the variability and the impact of various forcings on the SWW remains a significant area of investigation.

Earlier studies have provided evidence for a more northward location of the SWW during glacial periods (Lamy et al., 2004; Kaiser et al., 2005). Toggweiler et al. (2006) postulated feedback mechanisms involving the Southern Ocean CO_2 air-sea gas exchanges, global temperature and position of SWW whereby cooler climates would correspond to a more equatorward location of the SWW. Driving mechanisms and dynamics behind the variability in SWW are still unclear. Changes in seasonal insolation might also have caused a general strengthening and equatorward shift of the SWW during the late Holocene (Markgraf et al., 1992; Lamy et al., 2001; Jenny et al., 2003).

Another significant forcing that influences climate on decadal to millennial timescales is solar activity (e.g. Haigh, 1996; Cubasch et al., 1997; Bond et al., 2001; Versteegh, 2005; Spangehl et al., 2010), which could also be a potential driver for SWW variability. Van Geel et al. (2000) proposed solar activity as one of the possible factors for a shift in atmospheric circulation during the late Holocene around 2700 years BP. The abrupt decrease in solar activity during this period might have acted as a trigger for the glacier advancement towards the equator due to an equatorward shift of climatic zones along with the SWW (Van Geel et al., 2000). Solar-induced changes in stratospheric ozone through enhanced variability in the ultraviolet part of the solar spectrum were a postulated factor for shifting the SWW by influencing the tropospheric subtropical westerly jet through dynamic relations between the atmospheric layers (Haigh, 1996).

The potential role of solar forcing in Southern Hemisphere mid-latitude climate variability on the quasi-decadal timescale has been investigated by Thresher (2002) using observational data from the instrumental period. For longer timescales, the study of proxy data from natural archives is necessary. Here, we investigate the influence of centennial-scale total solar irradiance (TSI) variations on the SWW using proxy data from the late Holocene in combination with sensitivity experiments employing a state-of-the-art comprehensive global climate model. The results will lead us to the suggestion that equatorward (southward) shifts of the SWW occurred during centennial-scale periods of lower (higher) solar activity.

2 Proxy evidence for solar-forced SWW shifts

The mid-latitudes of Chile exhibit an extreme north-south precipitation gradient which is controlled by the latitudinal position of the SWW. Furthermore, local correlation analyses have shown that, in central and southern Chile, rainfall on the western side of the Andes is almost entirely determined by the westerlies (Garreaud, 2007). Therefore, any paleoclimate proxy that is primarily controlled by precipitation changes is a potential recorder of past changes of the SWW in this region. High-accumulation rate marine sediment core GeoB3313-1 from the Chilean continental slope (41° S, 74.45° W) provides a mid-to-late Holocene record of rainfall variability through its iron content (Lamy et al., 2001). Figure 1 shows the core location and illustrates the relation between precipitation over the region and zonal surface wind. During austral winter, the northern margin of the westerly wind belt is shifted towards the equator resulting in enhanced precipitation over the catchment represented by the core (Fig. 1a). Conversely, during austral summer, the westerlies tend to get intensified further south resulting in a decreased precipitation over the catchment represented by the core (Fig. 1b). Given the strong influence of the SWW on the precipitation pattern, the iron data from core GeoB3313-1, which primarily reflect changes in paleoprecipitation, are likely to provide information on the SWW position. A higher content of iron in the core region indicates drier conditions probably due to southward shifted SWW, whereas a lower iron concentration is indicative of wetter conditions suggesting northward shifted SWW (Lamy et al., 2001).

In order to find a possible correlation of the iron record with Holocene solar forcing, we use reconstructions of solar activity based on ^{14}C (Solanki et al., 2004) and ^{10}Be (Vonmoos et al., 2006). Comparison of the records suggests a possible link between the sun's radiative output and the inferred shift of the SWW, indicating an equatorward (southward) displacement of the SWW during periods of lower (higher) solar activity during the last 3000 years (Fig. 2). Linear correlations over this time interval are significant for both solar reconstructions. While the Pearson correlation coefficient (r) for

^{14}C is relatively small (but statistically significant), the large correlation coefficient for ^{10}Be would suggest that ca. 20% (i.e. r^2) of late Holocene rainfall and hence SWW variability is attributable to solar forcing.

3 Model evidence for solar-forced SWW shifts

To investigate the effect of TSI on the SWW we use the comprehensive global climate model CCSM3 (Community Climate System Model version 3). NCAR's (National Centre for Atmospheric Research) CCSM3 is a state-of-the-art fully coupled model, composed of four separate components representing atmosphere, ocean, land and sea-ice (Collins et al., 2006). Here, we employ the low-resolution version described in detail by Yeager et al. (2006). In this version the resolution of the atmospheric component is given by T31 (3.75° transform grid), with 26 layers in the vertical, while the ocean has a nominal resolution of 3° (like the sea-ice component) with a vertical resolution of 25 levels.

The control run was carried out with a solar constant of 1365 W/m^2, while solar sensitivity experiments were carried out with a lower solar irradiance value of 1363 W/m^2 (i.e. reduction by 0.15%). Pre-industrial boundary conditions were applied in all simulations following the protocol established by the Paleoclimate Modelling Intercomparison Project, Phase II (Braconnot et al., 2007). This forcing represents the average conditions of the late Holocene before the significant impact of humans, rather than a specific date, and it accounts for concentrations of greenhouse gases (e.g. CO_2 concentration of 280 ppmv), ozone, sulphate and carbonaceous aerosols (Otto-Bliesner et al., 2006). After a 600-year spin-up, the control simulation (Merkel et al., 2010) was run for another 150 years, while three sensitivity runs with reduced solar constant were branched off at model years 600, 640 and 680, respectively. Each sensitivity run was integrated for 70 years, which is a typical timescale for the duration of solar "Grand minima" like the Wolf (1280–1350 AD), Spörer (1450–1550 AD) or Maunder (1645–1715 AD) Minimum. Our choice of TSI reduction of 2 W/m^2 between solar maximum and solar minimum in the model experiments is consistent with recent observation and physics based estimates (Steinhilber et al., 2009).

The difference between sensitivity and control run (i.e. low minus high TSI simulation for a specific 70-year interval) was calculated for each ensemble member and, subsequently, the ensemble mean was taken and subjected to statistical analyses using a Student's t-test. Figure 3a shows the 70-year-averaged annual mean zonal wind anomaly at 1000 hPa, in response to lower solar activity, for the ensemble mean. The model results suggest a shift of surface wind fields towards the equator in response to TSI reduction, consistent with the proxy evidence discussed above. Figure 3b depicts the zonally averaged annual mean zonal wind anomaly as a function of latitude and height, showing that the equatorward SWW shift takes place at all levels in the troposphere. The wind anomaly patterns exhibit opposite signs for the different seasons, i.e. for lower solar activity, the SWW experience an equatorward shift during austral summer and a poleward shift during austral winter (Fig. 4). However, it is the austral summer pattern (December/January/February) which dominates the annual mean distribution, as can be seen by comparing Figs. 3 and 4.

An equatorward shift of the SWW should result in increased precipitation over central Chile. Since a low-resolution version of CCSM3 has been used here, local features and in particular orographic rainfall at the Andes cannot be fully captured. The model still simulates positive precipitation anomalies over the Chilean regions of enhanced westerlies, albeit with a very small magnitude and statistically not significant at the 0.1 significance level according to a t-test (not shown). We finally note that a direct comparison between model output and proxy data from a specific location is also hampered by the fact that the summer SWW in CCSM3 are biased towards north (see www.ccsm.ucar.edu/experiments/ccsm3.0/atm/b30.031-obs_801-820/set4/set4_DJF_U_NCEP_obsc.png for the present-day control run).

4 Discussion

Even though the influence and importance of the SWW on a global scale has been identified in previous studies, little is known about its variability and forcings. Our correlation analysis between the GeoB3313-1 iron record and solar activity reconstructions suggests a significant influence of the sun's radiative output on the position of the SWW for the last 3000 years on a (multi-)centennial timescale. For the early and mid-Holocene (i.e. prior to 3000 years BP), however, the correlation is close to zero (not shown). This incongruity might be an artifact due to, e.g. dating uncertainties in the deeper section of core GeoB3313-1. It might also be that, due to a generally more southward position of the SWW's northern margin in the early and mid-Holocene (Markgraf et al., 1992; Lamy et al., 2001; Jenny et al., 2003), the core was not at an ideal location to record centennial-scale fluctuations in the SWW. On the other hand, one can also conjecture that the westerly wind system was indeed less sensitive to variations in solar activity during the early and mid-Holocene due to different orbital forcing. The latter hypothesis is testable by model simulations and will be the subject of future work.

The climate model used in this study has a poorly resolved stratosphere and does not include feedbacks associated with the effect of enhanced variability in the ultraviolet part of the solar spectrum on photochemical dissociation rates and the subsequent impact on stratospheric ozone (Haigh, 1999; Rind et al., 2008). Instead, applied changes in TSI mostly affect the climate system through shortwave absorption by the surface (note that almost 70% of shortwave radiation that enters the atmosphere and is not reflected back to space, is absorbed at the surface), whereas less direct heating by solar radiation takes place at higher levels of the atmosphere. Therefore, the climate response in our experiment is mainly through ”bottom-up mechanisms” (Meehl et al., 2009). By contrast, a “top-down” mechanism, which influences the troposphere via stratospheric ozone responses to variations in ultraviolet radiation, has been proposed by Haigh (1996). In her model, increase in ultraviolet radiation and resulting rise in

CPD

6, 369–384, 2010

Solar-forced shifts of the Southern Hemisphere Westerlies

V. Varma et al.

ozone concentration, induced heating in the lower stratosphere during the Southern Hemisphere summer. As a consequence, strengthened stratosphere easterly winds caused the tropospheric subtropical westerly jets to move poleward, the tropical Hadley cell to broaden, and the SWW to move southward. "Bottom-up" and "top-down" mechanisms are not mutually exclusive. The model by Haigh (1996) used fixed sea surface temperatures and, hence, is unable to simulate "bottom-up" mechanisms that are important in our coupled climate model. We therefore suggest that the processes linking solar variability to the SWW in the two different models may complement each other, thus leading to a stronger total response than given by each individual process alone.

Understanding the exact dynamics behind the SWW shift in our simulations is beyond the scope of the present study and will be the subject of future work. We note, however, that a southward shift of the SWW in response to enhanced TSI is consistent with the general notion of an expansion of the Hadley cell and a poleward displacement of extra-tropical circulation patterns with increased mean temperature (Frierson et al., 2007). Moreover, a "bottom-up" response for peaks in solar forcing, involving a strengthening of the Hadley circulation through air-sea interactions, has been suggested by Meehl et al. (2008 and 2009).

5 Conclusions

Evidence for a significant solar influence on climate is rapidly growing based on natural archives from the Northern Hemisphere. Proxy data from the Southern Hemisphere, however, are notoriously sparse (Versteegh, 2005). Here, we presented proxy and model evidence that centennial-scale variability in the position of the SWW was significantly influenced by fluctuations in solar activity during the past 3000 years. Periods of lower solar activity were associated with annual-mean equatorward shifts of the SWW, whereas periods of higher solar activity were linked to annual-mean poleward displacements of the SWW. Given the significant correlation between solar activity and SWW, as suggested by the ^{10}Be (Vonmoos et al., 2006) and GeoB3313-3 iron records (Lamy et al., 2001), we propose that the role of the sun in modifying Southern Hemisphere tropospheric circulation patterns has probably been underestimated in model simulations of past climate change. More investigations are yet to be carried out to shed light on possible mechanisms that explain the relation between solar activity and westerly wind variability.

Acknowledgements. This work was funded through the DFG (Deutsche Forschungsgemeinschaft) Priority Programme "INTERDYNAMIK" and through the DFG Research Center/Excellence Cluster "The Ocean in the Earth System". We are indebted to Jürg Beer and Sami Solanki for providing the solar activity reconstructions as well as to Bruce Briegleb and Bette Otto-Bliesner for providing CCSM3 pre-industrial boundary conditions. We thank Axel Timmermann for stimulating discussions. CCSM3 simulations were performed on the IBM supercomputer of the Norddeutscher Verbund für Hoch- und Höchstleistungsrechnen (HLRN).

PAGES PAST GLOBAL CHANGES

The publication of this article was sponsored by PAGES.

References

Anderson, R. F., Ali, S., Bradtmiller, L. I., Nielsen, S. H. H., Fleisher, M. Q., Anderson, B. E., and Burckle, L. H.: Wind-Driven Upwelling in the Southern Ocean and the Deglacial Rise in Atmospheric CO_2, Science, 323, 1443–1448, 2009.

Biastoch, A., Böning, C. W., Schwarzkopf, F. U., and Lutjeharms, J. R. E.: Increase in Agulhas leakage due to poleward shift of Southern Hemisphere westerlies, Nature, 462, 495–498, 2009.

Bond, G., Kromer, B., Beer, J., Muscheler, R., Evans, M. N., Showers, W., Hoffmann, S., Lotti-Bond, R., Hajdas, I., and Bonani, G.: Persistent Solar Influence on North Atlantic Climate During the Holocene, Science, 294, 2130–2136, 2001.

Braconnot, P., Otto-Bliesner, B., Harrison, S., Joussaume, S., Peterchmitt, J.-Y., Abe-Ouchi, A., Crucifix, M., Driesschaert, E., Fichefet, Th., Hewitt, C. D., Kageyama, M., Kitoh, A., Laîné, A., Loutre, M.-F., Marti, O., Merkel, U., Ramstein, G., Valdes, P., Weber, S. L., Yu, Y., and Zhao, Y.: Results of PMIP2 coupled simulations of the Mid-Holocene and Last Glacial Maximum – Part 1: experiments and large-scale features, Clim. Past, 3, 261–277, 2007, http://www.clim-past.net/3/261/2007/.

Collins, W. D., Bitz, C. M., Blackmon, M. L., Bonan, G. B., Bretherton, C. S., Carton, J. A., Chang, P., Doney, S. C., Hack, J. J., Henderson, T. B., Kiehl, J. T., Large, W. G., McKenna, D. S., Santer, B. D., and Smith, R. D.: The Community Climate System Model Version 3 (CCSM3), J. Climate, 19, 2122–2143, 2006.

Cubasch, U., Voss, R., Hegerl, G. C., Waszkewitz, J., and Crowley, T. J.: Simulation of the influence of solar radiation variations on the global climate with an ocean-atmosphere general circulation model, Clim. Dynam., 13, 757–767, 1997.

Frierson, D. M. W., Lu, J., and Chen, G.: Width of the Hadley cell in simple and comprehensive general circulation models, Geophys. Res. Lett., 34, L18804, doi:10.1029/2007GL031115, 2007.

Garreaud, R. D.: Precipitation and Circulation Covariability in the Extratropics, J. Climate, 20, 4789–4797, 2007.

Haigh, J. D.: The impact of solar variability on Climate, Science, 272, 981–984, 1996.

Haigh, J. D.: Modelling the impact of solar variability on climate, J. Atmos. Sol-Terr. Phy., 61, 63–72, 1999.

Jenny, B., Wilhelm, D., and Valero-Garcés, B. L.: The Southern Westerlies in Central Chile: Holocene precipitation estimates based on a water balance model for Laguna Aculeo (33°50′ S), Clim. Dynam., 20, 269–280, 2003.

Kaiser, J., Lamy, F., and Hebbeln, D.: A 70-kyr sea surface temperature record off southern Chile (Ocean Drilling Program Site 1233), Paleoceanography, 20, PA4009, doi:10.1029/2005PA001146, 2005.

Kalnay, E., Kanamitsu, M., Kistler, R., Collins, W., Deaven, D., Gandin, L., Iredell, M., Saha, S., White, G., Woollen, J., Zhu, Y., Leetmaa, A., Reynolds, R., Chelliah, M., Ebisuzaki, W., Higgins, W., Janowiak, J., Mo, K. C., Ropelewski, C., Wang, J., Jenne, R., and Joseph, D.: The NCEP/NCAR 40-Year Reanalysis Project, B. Am. Meteorol. Soc., 77, 437–471, 1996.

Kuhlbrodt, T., Griesel, A., Montoya, M., Levermann, A., Hofmann, M., and Rahmstorf, S.: On the driving processes of the Atlantic meridional overturning circulation, Rev. Geophys., 45, RG2001, doi:10.1029/2004RG000166, 2007.
Lamy, F., Hebbeln, D., Röhl, U., and Wefer, G.: Holocene rainfall variability in southern Chile: a marine record of latitudinal shifts of the Southern Westerlies, Earth Planet. Sc. Lett., 185, 369–382, 2001.
Lamy, F., Kaiser, J., Ninnemann, U., Hebbeln, D., Arz, H. W., and Stoner, J.: Antarctic Timing of Surface Water Changes off Chile and Patagonian Ice Sheet Response, Science, 304, 1959–1962, 2004.
Markgraf, V., Dodson, J. R., Kershaw, P. A., McGlone, M. S., and Nicholls, N.: Evolution of late Pleistocene and Holocene climates in the circum-South Pacific land areas, Clim. Dynam., 6, 193–211, 1992.
Meehl, G. A., Arblaster, J. M., Branstator, G., and van Loon, H.: A coupled air-sea response mechanism to solar forcing in the Pacific region, J. Climate, 21, 2883–2897, 2008.
Meehl, G. A., Arblaster, J. M., Matthes, K., Sassi, F., and van Loon, H.: Amplifying the Pacific Climate System Response to a Small 11-Year Solar Cycle Forcing, Science, 325, 1114–1118, 2009.
Merkel, U., Prange, M., and Schulz, M.: ENSO variability and teleconnections during glacial climates, Quaternary Sci. Rev., 29, 86–100, 2010.
Mudelsee, M.: Estimating Pearson's correlation coefficient with bootstrap confidence interval from serially dependent time series, Math. Geol., 35, 651–665, 2003.
Otto-Bliesner, B. L., Tomas, R., Brady, E. C., Ammann, C., Kothavala, Z., and Clauzet, G.: Climate sensitivity of moderate- and low-resolution versions of CCSM3 to preindustrial forcings, J. Climate, 19, 2567–2583, 2006.
Rind, D., Lean, J., Lerner, J., Lonergan, P., and Leboissitier, A.: Exploring the stratospheric/tropospheric response to solar forcing, J. Geophys. Res-Atmos., 113, D24103, doi:10.1029/2008JD010114, 2008.
Shulmeister, J., Goodwin, I., Renwick, J., Harle, K., Armand, L., McGlone, M. S., Cook, E., Dodson, J., Hesse, P. P., Mayewski, P., and Curran, M.: The Southern Hemisphere westerlies in the Australasian sector over the last glacial cycle: a synthesis, Quatern. Int., 118–119, 23–53, 2004.
Sijp, W. P. and England, M. H.: Southern Hemisphere Westerly Wind Control over the Ocean's Thermohaline Circulation, J. Climate, 22, 1277–1286, 2009.

Solanki, S. K., Usoskin, I. G., Kromer, B., Schüssler, M., and Beer, J.: Unusual activity of the Sun during recent decades compared to the previous 11,000 years, Nature, 431, 1084–1087, 2004.

Spangehl, T., Cubasch, U., Raible, C. C., Schimanke, S., Körper, J., and Hofer, D.: Transient climate simulations from the Maunder Minimum to present day: Role of the Stratosphere, J. Geophys. Res.-Atmos., 115, D00I10, doi:10.1029/2009JD012358, 2010.

Steinhilber, F., Beer, J., and Fröhlich, C.: Total solar irradiance during the Holocene, Geophys. Res. Lett., 36, L19704, doi:10.1029/2009GL040142, 2009.

Thresher, R. E.: Solar correlates of Southern Hemisphere mid-latitude climate variability, Int. J. Climatol., 22, 901–915, 2002.

Toggweiler, J. R. and Samuels, B.: Effect of Drake Passage on the global thermohaline circulation, Deep-Sea Res. Pt 1., 42, 477–500, 1995.

Toggweiler, J. R., Russel, J. L., and Carson, S. R.: Midlatitude westerlies, atmospheric CO_2 and climate change during the ice ages, Paleoceanography, 21, PA2005, doi:10.1029/2005PA001154, 2006.

van Geel, B., Heusser, C. J., Renssen, H., and Schuurmans, C. J. E.: Climatic change in Chile at around 2700 BP and global evidence for solar forcing: a hypothesis, Holocene, 10, 659–664, 2000.

Versteegh, G. J. M.: Solar forcing of climate. 2: Evidence from the Past, Space Sci. Rev., 120, 243–286, 2005.

Vonmoos, M., Beer, J., and Muscheler, R.: Large variations in Holocene solar activity: Constraints from ^{10}Be in the Greenland Ice Core Project ice core, J. Geophys. Res.-Space, 111, A10105, doi:10.1029/2005JA011500, 2006.

Yeager, S. G., Shields, C. A., Large, W. G., and Hack, J. J.: The low-resolution CCSM3, J. Climate, 19, 2545–2566, 2006.

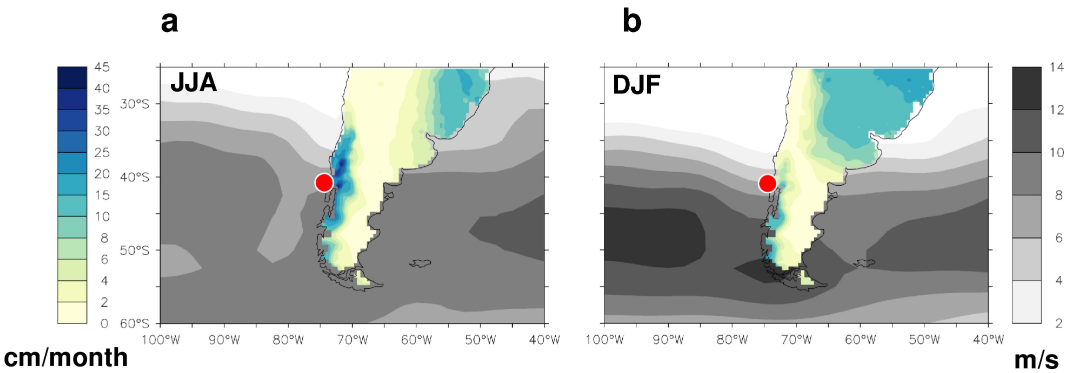

Fig. 1. Long-term climatological distribution of precipitation over land and 1000 hPa zonal wind over oceans in the region of marine sediment core GeoB3313-1 located at 41°S (red dot) for **(a)** austral winter (June/July/August) and **(b)** austral summer (December/January/February). During winter, surface winds (shown in grey shades) move towards the north, resulting in enhanced precipitation (shown in bluish shades) over the catchment represented by the core. During summer, the winds are more confined towards the south, resulting in decreased precipitation over the catchment represented by the core. Data: University of Delaware precipitation (http://climate.geog.udel.edu/~climate/), NCEP-NCAR reanalysis winds (Kalnay et al., 1996).

CPD
6, 369–384, 2010

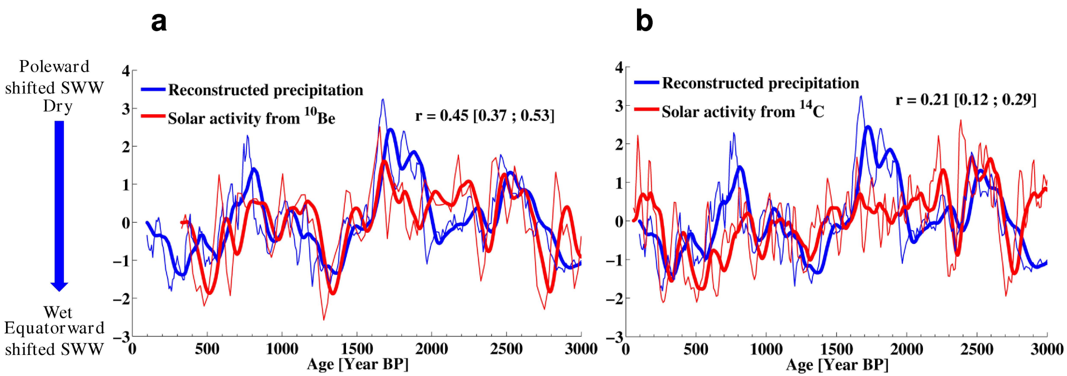

Fig. 2. Reconstructions of precipitation and hence position of the SWW (based on the GeoB3313-1 iron record) versus solar activity for the late Holocene. **(a)** Solar activity based on ^{10}Be (Vonmoos et al., 2006), **(b)** solar activity based on ^{14}C (Solanki et al., 2004). Time series are linearly detrended and standardized. The bold curves show 100-year running means and thin curves show the unsmoothed data. A lower content of iron stands for wetter conditions, suggesting northward shifted SWW (Lamy et al., 2001). Conversely, a higher content of iron reflects drier conditions which are essentially due to southward shifted SWW. Pearson correlation coefficients (r) were calculated from the unsmoothed data. 95% confidence intervals (in brackets) were calculated using a bootstrap method, where autocorrelation has been taken into account (Mudelsee, 2003).

CPD
6, 369–384, 2010

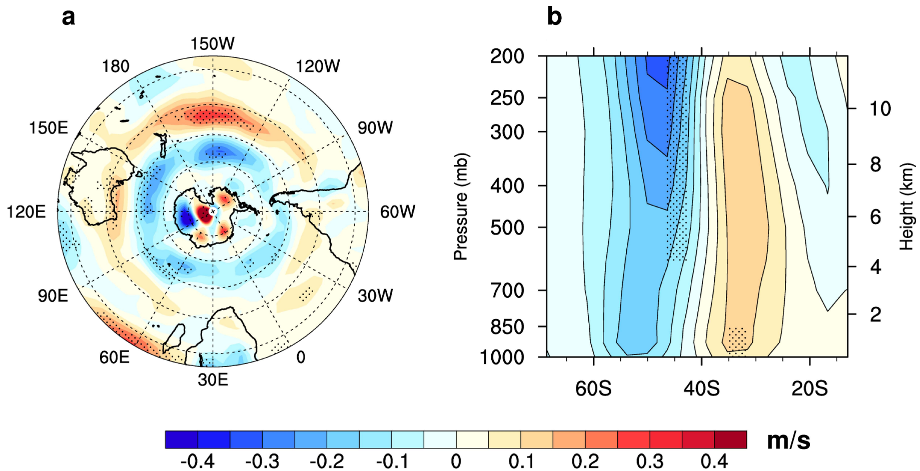

Fig. 3. Distribution of annual mean zonal wind anomaly (low minus high total solar irradiance) in the model ensemble mean, averaged over the entire 70-year interval of the solar forcing experiment. **(a)** Zonal wind anomaly in the Southern Hemisphere at 1000 hPa, showing the clear equatorward shift of SWW. **(b)** Zonally averaged zonal wind anomaly for the Southern Hemisphere showing that the equatorward shift of SWW is pronounced even at upper levels of the troposphere. Stippling indicates significance of the anomaly at the 0.1 level (applying a Student's t-test).

CPD
6, 369–384, 2010

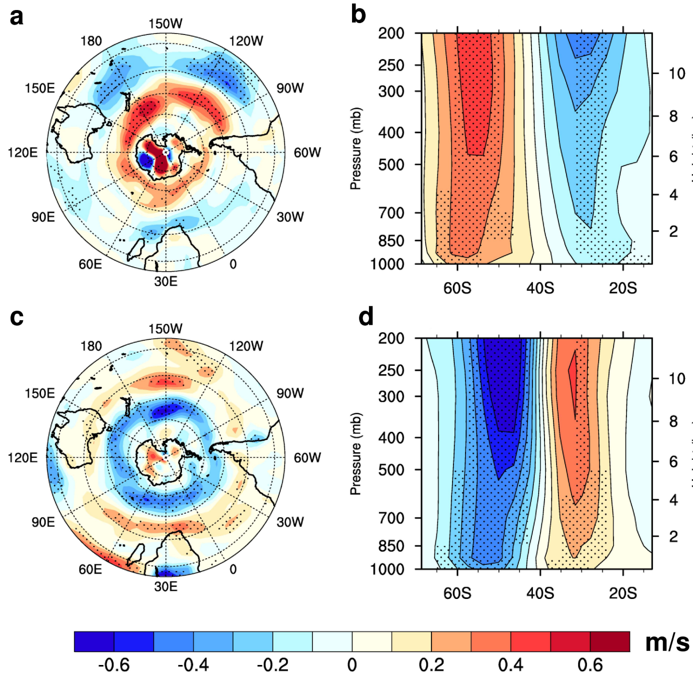

Fig. 4. Seasonal distribution of zonal wind anomaly (low minus high total solar irradiance) in the model ensemble mean, averaged over the entire 70-year interval of the solar forcing experiment. **(a)** and **(c)** Zonal wind anomaly in the Southern Hemisphere at 1000 hPa for austral winter (June/July/August) and austral summer (December/January/February), respectively. The wind anomaly patterns exhibit opposite signs for the different seasons, i.e. for lower solar activity, the SWW experience an equatorward shift during austral summer and a poleward shift during austral winter. **(b)** and **(d)** Zonally averaged zonal wind anomaly for the Southern Hemisphere for austral winter (June/July/August) and austral summer (December/January/February), respectively. Stippling indicates significance of the anomaly at 0.1 level (applying a Student's t-test).